UNIVERSITEIT
AMSTERDAM

VU Research Portal

Connectome-Based Patterns of First-Episode Medication-Naïve Patients With Schizophrenia

Cui, Long-Biao; Wei, Yongbin; Xi, Yi-Bin; Griffa, Alessandra; De Lange, Siemon C; Kahn, René S; Yin, Hong; Van den Heuvel, Martijn P

document version
Publisher's PDF, also known as Version of record

document license
Article 25fa Dutch Copyright Act

Link to publication in VU Research Portal

Download date: 27. May. 2021

Connectome-Based Patterns of First-Episode Medication-Naïve Patients With Schizophrenia

Long-Biao Cui[1,2,4,6,ⓘ], Yongbin Wei[2,3,6], Yi-Bin Xi[1], Alessandra Griffa[3,ⓘ], Siemon C. de Lange[3], René S. Kahn[2], Hong Yin[*,1,6], and Martijn P. van den Heuvel[2,3,5,6]

[1]Department of Radiology, Xijing Hospital, Fourth Military Medical University, Xi'an, China; [2]Department of Psychiatry, Brain Center Rudolf Magnus, University Medical Center Utrecht, Utrecht, The Netherlands; [3]Connectome Lab, Department of Complex Trait Genetics, Center for Neurogenomics and Cognitive Research, Amsterdam Neuroscience, Vrije Universiteit Amsterdam, Amsterdam, The Netherlands; [4]School of Medical Psychology, Fourth Military Medical University, Xi'an, China; [5]Department of Clinical Genetics, Amsterdam Neuroscience, Amsterdam University Medical Center, Amsterdam, The Netherlands

[6] These authors contributed equally to this work.

*To whom correspondence should be addressed: Department of Radiology, Xijing Hospital, Fourth Military Medical University, No. 127 West Changle Road, Xi'an 710032, China; tel: 86-29-84775424, fax: 86-29-84775421, e-mail: yinhong@fmmu.edu.cn.

Emerging evidence indicates that a disruption in brain network organization may play an important role in the pathophysiology of schizophrenia. The neuroimaging fingerprint reflecting the pathophysiology of first-episode schizophrenia remains to be identified. Here, we aimed at characterizing the connectome organization of first-episode medication-naïve patients with schizophrenia. A cross-sectional structural and functional neuroimaging study using two independent samples (principal dataset including 42 medication-naïve, previously untreated patients and 48 healthy controls; replication dataset including 39 first-episode patients [10 untreated patients] and 66 healthy controls) was performed. Brain network architecture was assessed by means of white matter fiber integrity measures derived from diffusion-weighted imaging (DWI) and by means of structural-functional (SC-FC) coupling measured by combining DWI and resting-state functional magnetic resonance imaging. Connectome rich club organization was found to be significantly disrupted in medication-naïve patients as compared with healthy controls ($P = .012$, uncorrected), with rich club connection strength ($P = .032$, uncorrected) and SC-FC coupling ($P < .001$, corrected for false discovery rate) decreased in patients. Similar results were found in the replication dataset. Our findings suggest that a disruption of rich club organization and functional dynamics may reflect an early feature of schizophrenia pathophysiology. These findings add to our understanding of the neuropathological mechanisms of schizophrenia and provide new insights into the early stages of the disorder.

Key words: schizophrenia/first-episode/human conne ctome/rich club/MRI

Introduction

Recent analyses of brain structure[1,2] and function[3] have indicated that disruptions in brain network organization may play an important role in schizophrenia. These findings suggest that the disorder may involve a deficit of neural communication efficacy and information integration in the brain's connectivity network.[4]

A network attribute of particular interest in the investigation of schizophrenia is the brain's "rich club."[5] The rich club describes a set of densely connected hub regions, suggested to provide an anatomical backbone for functional information communication and integration.[6,7] Network studies have suggested that chronic schizophrenia is characterized by an abnormal rich club organization, with reduced brain connectivity among hub regions.[8] Studies have reported rich club abnormalities in schizophrenia and psychosis patients,[9–11] as well as in subjects at high risk for the disorder[12] and general psychosis,[13] suggesting that rich club disorganization may be a central aspect of the neurobiological background of psychotic disorders.

One of the obstacles in identifying neuroimaging markers of schizophrenia pathophysiology is the clinical heterogeneity inherent to the nature of the disorder,[14] underscoring the importance of minimizing confounding factors such as prior therapeutic exposure and the potential influence of chronicity. An important step in the investigation of neuroimaging signatures of schizophrenia is thus to study first-episode, medication-naïve patients whose medical history is short and therapy is absent. Here, we examined the connectome structure in first-episode (with the majority medication-naïve) schizophrenia patients

using diffusion-weighted imaging (DWI) and resting-state functional magnetic resonance imaging (rs-fMRI).

Methods

Participants

Two independent datasets of first-episode schizophrenia patients were recruited at the Department of Psychiatry, Xijing Hospital. This study was approved by the local ethics committee and all participants (or their parents for those under age of 18 years) gave written informed consent after a full description of the aims and design of the study. Table 1 and the supplementary methods provide further details on the two datasets.

The resulting principal dataset included 42 patients with first-episode schizophrenia (all untreated, medication-naïve patients, table 1) and 48 controls.[15,16] The structural clinical interview for Diagnostic and Statistical Manual of Mental Disorders, Fourth Edition, Text Revision (DSM-IV-TR) was used, and consensus diagnoses were made using the available data by 2 senior psychiatrists. Each patient was assessed at the time of scanning using the Positive and Negative Syndrome Scale (PANSS).

The replication dataset included 39 first-episode patients with schizophrenia. This set included 10 untreated, medication-naïve patients, 29 patients with no more than 2 weeks of cumulative exposure to antipsychotics (see table 1), and 66 age- and gender-matched controls. Neuroimaging data of the control subjects have been investigated in a prior study.[16] Patients were diagnosed according to the DSM, Fifth Edition (DSM-5) and assessed at the time of imaging using the PANSS. In the

Table 1. Demographical and Clinical Data of Participants

Characteristic	Principal dataset			Replication dataset		
	Patients (n = 42)	HCs (n = 48)	P-values	Patients (n = 39)	HCs (n = 66)	P-values
Sociodemographic						
Age, years	25.0 ± 6.4	26.3 ± 4.1	.24[a]	24.6 ± 6.6	26.7 ± 5.6	.09[a]
Gender, male/female	24/18	22/26	.28[b]	21/18	39/27	.60[b]
Ethnicity, Han/others	42/0	48/0		39/0	66/0	
Education level, year	13.3 ± 1.7	14.5 ± 2.0	.004[c]	11.9 ± 3.3	16.0 ± 3.4	< .001[c]
Clinical						
Inpatients/outpatients	41/1	NA		37/2	NA	
Duration of illness, month[d]	11.3 ± 14.6	NA		13.7 ± 23.8	NA	
PANSS total score	97.0 ± 18.5	NA		84.1 ± 12.0	NA	
PANSS positive score	24.1 ± 8.3	NA		22.0 ± 4.7	NA	
PANSS negative score	23.5 ± 8.3	NA		19.2 ± 6.1	NA	
PANSS general psychopathology score	49.5 ± 8.9	NA		42.8 ± 7.3	NA	
Medical						
Medication, no/yes	42/0	NA		10/29	NA	
Risperidone	NA	NA		16	NA	
Risperidone and paliperidone	NA	NA		1	NA	
Risperidone and haloperidol	NA	NA		1	NA	
Risperidone and clozapine	NA	NA		1	NA	
Olanzapine	NA	NA		7	NA	
Paliperidone	NA	NA		2	NA	
Amisulpride	NA	NA		1	NA	
Duration of treatment, day	NA	NA		4.3 ± 4.5	NA	
Dose equivalent, mg/day[e]	NA	NA		5.5 ± 5.0	NA	

Note: HCs, healthy controls; NA, not applicable; PANSS, Positive and Negative Syndrome Scale.
[a]Two sample *t*-test.
[b]Chi-square test.
[c]Wilcoxon Rank Sum test was performed due to the non-normal distribution of samples. The medians of education years were statistically different between two groups.
[d]Duration of illness was determined from onset of disease until first meeting diagnosis.
[e]Antipsychotic dose equivalent to olanzapine based on defined daily doses method (WHO Collaborating Centre for Drug Statistics Methodology, 2014).

main text, we report results obtained for the 10 untreated, medication naïve patients. Results relative to the whole replication dataset of 39 patients are reported in the supplementary results.

Image Acquisition and Preprocessing

High-resolution T1-weighted MRI, DWI, and rs-fMRI data were obtained for both cohorts. Specific scanning parameters are shown in supplementary table 1. Data preprocessing steps[8] included parcellation of the cortex into 68 regions according to the Desikan Killiany atlas[17] by applying the FreeSurfer (version 5.3.0) pipeline (https://surfer.nmr.mgh.harvard.edu) on the T1-weighted images. Analyses based on 114 and 219 region parcellations[18] showed similar results (see supplementary results). White matter fiber tracts were reconstructed from DWI images using the following procedure.[19] The 64 diffusion-weighted volumes ($b = 1000$ s/mm^2) and the obtained $b = 0$ volume were realigned and corrected for small head movements and gradient-induced distortions.[20] The diffusion profile within each voxel was reconstructed using generalized q-sampling imaging (GQI),[21] and fractional anisotropy (FA) maps were computed from fitting a single tensor.[22] White matter tracts were reconstructed using deterministic tractography using Fiber Assignment by Continuous Tracking (FACT).[23] Deterministic tractography has been shown to be a suitable method for reconstructing the connectome by means of the use of simulated connectome phantoms[24] and by means of comparison to animal tract-tracing data.[25,26] Eight streamline seeds were started within each white matter voxel and tracking continued until the streamline reached a voxel of low FA (<0.1), exited the white matter mask, or made a sharp turn (>45°).

rs-fMRI processing included volumes' realignment, coregistration to T1-weighted image, detrending, regression for nuisance signals (including 6 head motion parameters, ventricle, and white matter signals), motion scrubbing (framewise displacement [FD] > 0.25, dynamic variability [DVARS] > 1.5),[27] and band-pass filtering (0.01–0.1 Hz). Results obtained from rs-fMRI data including global signal regression are reported in supplementary results.

Further details on data preprocessing procedures are described in the supplementary methods.

Brain Network Construction

Structural Networks. Structural networks were constructed for each subject by combining the collection of the reconstructed tractography streamlines with the cortical parcellation (see supplementary methods). Network nodes were defined as the parcellated 68 cortical regions and connected by network edges when linked by reconstructed streamlines, with the number of streamlines (NOS) taken as connection weight of the connecting edge. Streamline volume density (SD) obtained by dividing the NOS by the average cortical volume of the connected regions was also examined to correct for potential effects of changes in cortical volume.[5,28] FA was also examined, providing information on microstructural organization of white matter connections (supplementary results). The reconstructed network was not thresholded and all analyses were performed based on the weighted networks as advised.[29,30]

Functional Networks. Regional time series were extracted from the preprocessed fMRI data by averaging the time series of all voxels within a cortical region. Interregional functional connectivity was calculated as the Pearson's correlation coefficient between the regional time series of all the 68 cortical regions (see supplementary methods for details). Structural and functional connectivity networks as constructed and analyzed in the current study are available for download at http://www.connectomelab.org.

Graph Theoretical Metrics

Global Network Structure. Graph theoretical metrics were calculated to characterize the network organization of the anatomical brain network. Network analysis included the computation of connectivity strength, network density, clustering coefficient, shortest path length, and normalized clustering coefficient γ and shortest path length λ with respect to 1000 randomized networks.[31] Graph metrics were computed on individual structural brain networks for NOS, SD, and FA weights (see supplementary methods for details).

Rich Club Organization. The weighted rich club coefficient $\Phi^w(k)$ was computed for a range of degree values k. $\Phi^w(k)$ was taken as the sum of the weights of the edges' subset $E_{>k}$, with $E_{>k}$ the set of edges between nodes with degree $> k$ in the network, divided by the sum of the weights of the strongest $|E_{>k}|$ connections of the whole network ($|.|$ indicating the cardinality of the set).[5,32] The normalized rich club coefficient $\Phi_{norm}(k)$ was computed as the ratio between $\Phi^w(k)$ in the brain network and the mean $\Phi_{random}(k)$ across 1000 random networks (see supplementary methods).

Functional Connectivity

Pearson's correlation was used to assess the level of structural-functional coupling (SC-FC coupling) between the strength of structural connectivity and the corresponding functional connectivity values across all reconstructed brain connections. Structural connectivity weights (NOS and SD) were resampled to Gaussian distributions.[28]

Statistical Analysis

Permutation testing (10 000 permutations) was used to assess alterations of rich club organization, connectivity

strength, SC-FC coupling, and other characteristic graph metrics. For each permutation, subjects were randomly assigned to two groups with the same size of the original patients and controls groups. Next, the between-group difference of the metric of interest between the randomized groups was computed to generate a null distribution. Based on the obtained null distribution, a *P*-value was assigned to assess the extent of alteration in the graph metric of interest in patients compared to controls,[8] according to the proportions of random permutations that exceeded the empirical value of the metric of interest. Pearson's correlations between graph metrics and clinical variables (e.g., PANSS scores, including positive scale, negative scale, general psychopathology scale, supplementary scores, and total scores) were computed. Results reaching an uncorrected *P* < 0.05 were reported as significant, with statistical rigidity tested by using the replication dataset.

Results

Global Graph Metrics

Patients and controls showed similar structural network density, with a mean (standard deviation) of 22.4% (1.9%) for patients and 22.1% (2.0%) for controls (*P* = .548).[30] No difference was observed between patients and controls on global graph metrics, suggesting a globally preserved topology of the brain structural network in untreated, first-episode schizophrenia patients.[33,34] Overall connectivity strength, network density, clustering coefficient, shortest path length (*P* > .310, 10 000 permutations), normalized clustering coefficient γ, and normalized shortest path length λ (*P* > .252, 10 000 permutations) were found to be similar between groups.

Rich Club Organization

Rich club organization was observed for both healthy controls and patients (normalized rich club coefficient Φ^w_{norm} curves of both groups are shown in figure 1A). Permutation analysis revealed a significantly decreased rich club coefficient in patients as compared with healthy controls (*P* = .012 for degree *k* ranging from 16 to 23, NOS weights, 10 000 permutations), suggesting a decreased connectivity level among rich club regions in first-episode untreated schizophrenia patients. Consistent findings were observed when including age and gender as covariates, *P* = .016, 10 000 permutations. Performing the analysis on the structural network weighted by SD also showed a significant reduction of rich club connectivity in patients compared to controls (*P* = .027, 10 000 permutations).

Rich Club, Feeder and Local Connections

Rich club regions were identified at a rich club threshold of degree *k* > 18 in the group-averaged structural network,
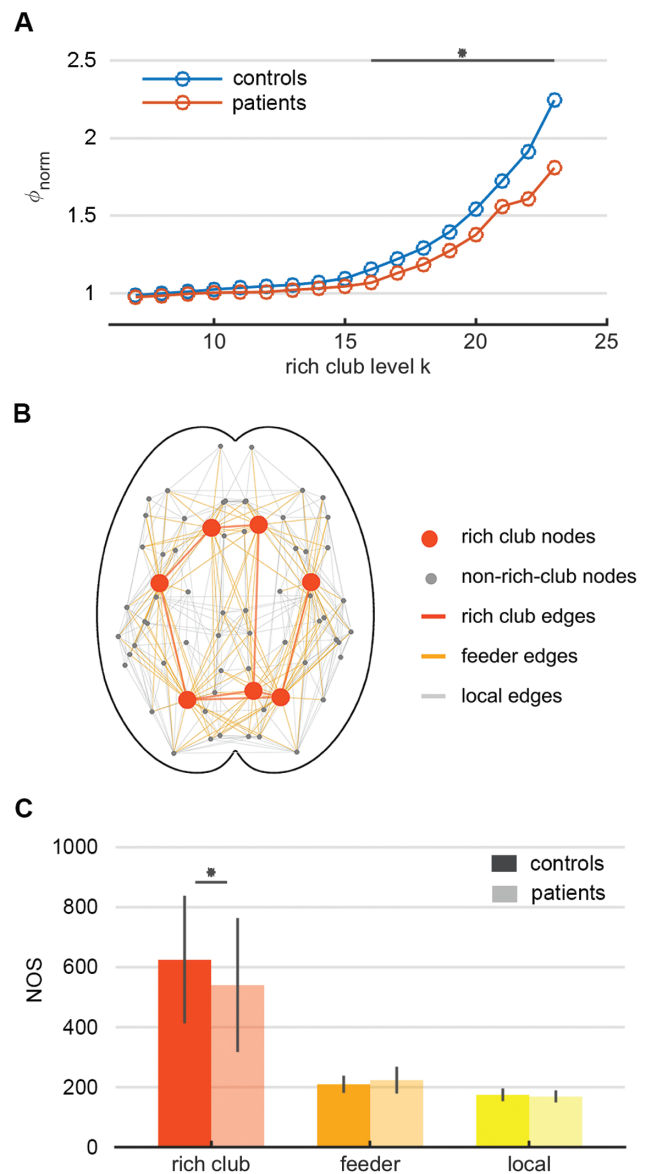

Fig. 1. (A) Decreased rich club coefficient in patients (red) as compared with healthy controls (blue) for degree *k* ranging from 16 to 23 (*P* = .012, 10 000 permutations, uncorrected). (B) Group-averaged structural network for healthy controls. Rich club regions (red) were identified by setting the threshold as degree >18, including bilateral superior frontal gyri, superior parietal lobules, insula, and left precuneus. Connections were classified into 3 categories: rich club (red), feeder (orange), and local (gray) connections. (C) Group-averaged connectivity strength (number of streamlines [NOS] weighted) of the rich club (red), feeder (orange), and local (yellow) connections in healthy controls (dark) and patients (light). Error bars represent one standard deviation. Patients showed decreased rich club connection density in comparison with healthy controls (*P* = .032, 10 000 permutations, uncorrected).

including bilateral superior frontal gyri, bilateral superior parietal lobules and insula, and left precuneus (figure 1B).[5,8] Results derived from a range of thresholds (i.e., *k* > 14–22) are shown in supplementary results. Rich club connectivity strength was found to be reduced in patients as compared

with controls (NOS, $P = .032$, 10 000 permutations). In contrast, no reduction was found for connections spanning between non-hub regions, i.e., feeder and local connections ($P = .962$ and $.105$, respectively; figure 1C), suggesting that the effect of brain disconnectivity was concentrated to rich club connections in patients. Effects remained significant when correcting for age and gender ($P = .031$, 10 000 permutations). Analyses of the SD also revealed decreased rich club connectivity in patients compared with healthy controls ($P = .016$, 10 000 permutations).

SC-FC Coupling

Overall FC strength (average of the FC matrix) was found to be similar across patients and controls ($P = .408$, 10 000 permutations), as was the FC strength of rich club, feeder, and local connections ($P > .526$, 10 000 permutations). Both patients and healthy controls demonstrated a positive correlation between overall SC and FC values, with a mean (standard deviation) SC-FC correlation coefficient of 0.271 (0.064) for patients and 0.272 (0.060) for controls (figure 2). SC-FC coupling was similar in patients compared to controls ($P = .461$, 10 000 permutations). Considering the distinct connection categories, a significantly reduced SC-FC coupling was detected for rich club connections in patients compared to controls ($P < .001$, 10 000 permutations, NOS-weighted), whereas no such difference in SC-FC coupling was found in feeder ($P = .865$) and local ($P = .414$) connections (figure 2). Similar effects were found when correcting for age and gender ($P < .001$, 10 000 permutations) and when using SC networks weighted by SD ($P < .001$, 10,000 permutations).

Correlation between Network Organization and Clinical Variables

No specific association between rich club connections' strength and symptom scores was observed. In patients, the strength of feeder connections was found to be negatively correlated with PANSS positive score (NOS, $r = -0.34$, $P = .030$) and total score ($r = -0.35$, $P = .022$), suggesting that patients with weaker feeder connections

may have more severe symptoms, especially with regard to positive symptoms. Strength of local connections was negatively correlated with PANSS positive score (NOS, $r = -0.32$, $P = .043$) and negative score (NOS, $r = -0.36$, $P = .019$) (figure 3). No specific correlation was found for SD connectivity.

Machine Learning Disease Classification

To explore the performance of classification using connectome measurements, we trained a quadratic support vector machine (SVM, see supplementary methods) based on structural connectivity strength and SC-FC coupling of rich club connections (see supplementary methods). Using five-fold cross-validation, we obtained a prediction accuracy of 73.3% (sensitivity = 76% and specificity = 71%; supplementary figure 4).

Replication Dataset

Patients' rich club effects were validated using the replication dataset. The cortical rich club was taken as the same set of regions as in the principal dataset (the two datasets showed high consistency in rich club organization, see supplementary results). Patients (10 medication-naïve patients; results for the full replication dataset including 29 additional patients with a short medication history are shown in supplementary results) again showed a significant reduction in rich club connectivity strength compared with healthy controls (NOS, $P = .021$, 10 000 permutations), with no difference observed in feeder ($P = .394$) or local ($P = .602$) connections (figure 4). Examining the SD of rich club connections showed similar results (rich club connectivity $P = .015$, 10 000 permutations). A marginal effect of reduced SC-FC coupling was observed for rich club connections ($P = .048$), with no effect for feeder ($P = .713$) and local ($P = .921$) connections.

Discussion

We investigated brain network organization in a sample of untreated, medication-naïve first-episode schizophrenia
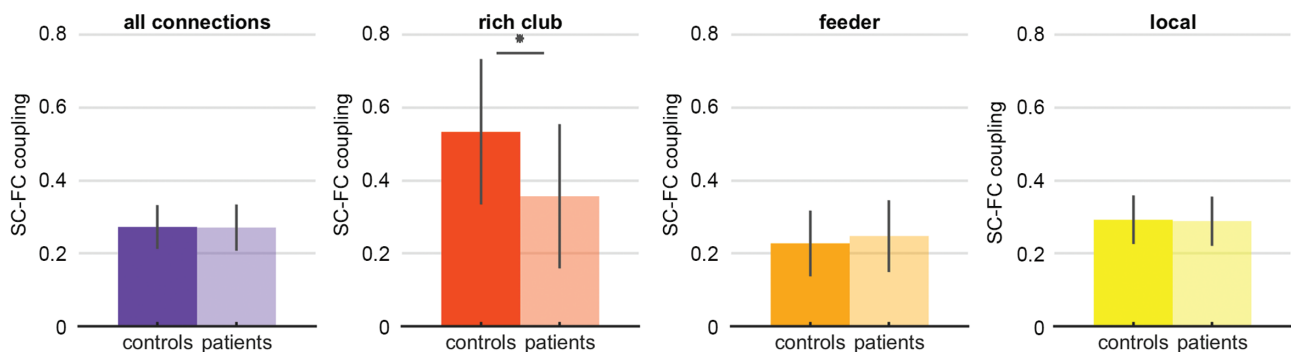

Fig. 2. SC-FC coupling in healthy controls (dark) and patients (light) for all connections, rich club connections ($P < .001$, 10 000 permutations, false discovery ratio [FDR] corrected), feeder connections (no effect), and local connections (no effect). Error bars represent one standard deviation and asterisk indicates significance.
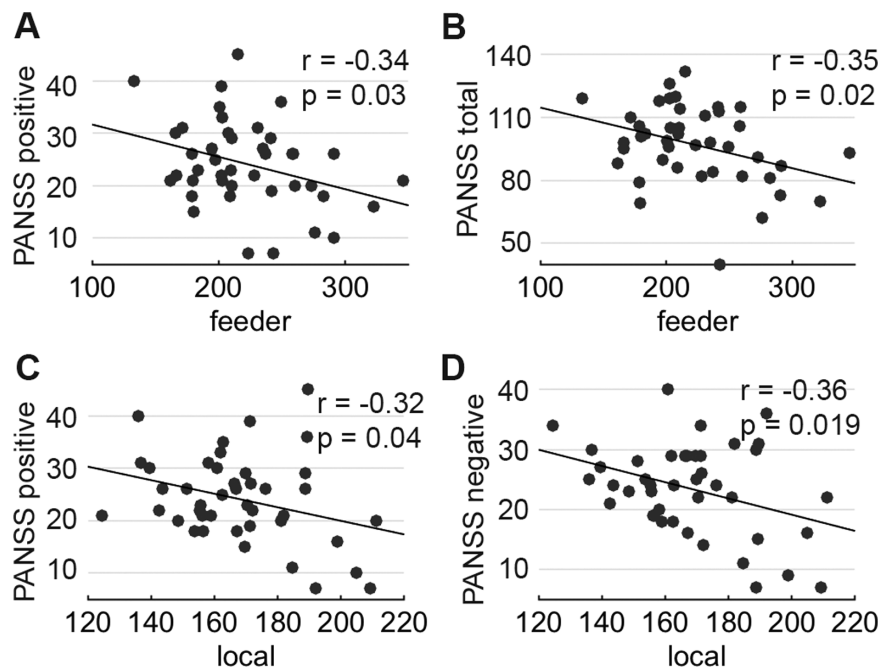
Fig. 3. Feeder connections (NOS) were negatively correlated with (A) PANSS positive score ($r = -0.34$, $P = .030$, uncorrected) and (B) total score ($r = -0.35$, $P = .022$, uncorrected) in patients. Local connections (NOS) were negatively correlated with (C) PANSS positive score ($r = -0.32$, $P = .043$, uncorrected) and (D) negative score ($r = -0.36$, $P = .019$, uncorrected).
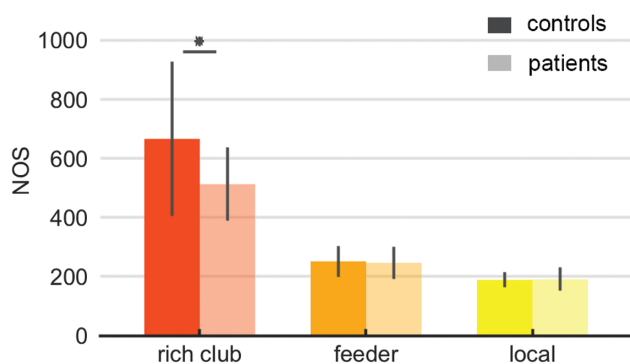

Fig. 4. Replication dataset. Patients showed reduced rich club connection strength compared with healthy controls (NOS, $P = .021$, 10 000 permutations, uncorrected). No difference was observed in feeder ($P = .394$) and local connections ($P = .602$). Error bars represent one standard deviation and asterisk indicates significance.

patients. Rich club organization and structure-function coupling of rich club connections were found to be altered in patients compared to controls, suggesting that rich club organization may be already impaired in the early stages of schizophrenia.

Previous studies have noted the potential influence of medication on brain network findings in schizophrenia.[11] In the current study, we took extra care to rule out medical and therapeutic effects by examining first-episode, medication-naïve patients. Our results suggest that the impairment of rich club organization directly relate to schizophrenia independently from possible confounding

factors, advancing our understanding of the disease mechanisms during the early stages of the disorder.

Previous studies have reported aberrant rich club connectivity and functional brain dynamics in European chronic schizophrenia patients.[8] Similar findings have been reported in a cohort of North American chronic schizophrenia patients[9] and, recently, in a large sample of Australian patients with schizophrenia or schizoaffective disorder.[10] Our study consolidates and extends these previous findings by showing an alteration of rich club organization in a cohort of Chinese patients and further underscores the cultural ubiquity of the biological underpinnings of schizophrenia.

Studies examining brain abnormalities in first-episode schizophrenia have reported fiber tract disruptions in the anterior limb of internal capsule,[35,36] cingulum,[37] and anterior corona radiate.[38–41] The rich club regions identified in this study, i.e., the bilateral superior frontal gyri, superior parietal lobules, and insula, as well as the precuneus, are located in parts of the brain interconnected by the abovementioned white matter tracts.[42,43] Rich club disruption is coherent with previous findings on schizophrenia patients[8,12] and suggests that brain network alterations may be concentrated around the centrally connected areas of the human brain.[10,42,43] In such highly connected fronto-parietal areas, myelination has been suggested to continue postnatally until the third decade of life,[44,45] which overlaps with the most frequent period of schizophrenia onset, occurring mostly in the early- to mid-20s for men and late-20s for women.[46] Therefore, our observed structural rich club findings in first-episode

patients may indirectly reflect an important neurodevelopmental feature of schizophrenia.

With converging evidence pointing to a rich club white matter impairment in both early and chronic stages of schizophrenia, a critical next step will be to determine and assess the potential value of these features in clinical applications. "Radiomics," defined as "the conversion of images to higher-dimensional data and the subsequent mining of these data for improved decision support,"[47] represents the next step in promoting the translation[48] of brain connectome-based features to diagnosis and prediction for schizophrenia. A radiomics analysis involves the high-throughput extraction of meaningful measures (such as rich club connectivity) from medical images to support clinical decision processes.[47] Previous studies have suggested that gray matter abnormalities in schizophrenia are frequent, but quite heterogeneous across patients,[49] potentially limiting the contribution of gray matter features as a single biomarker for the disorder. Using machine learning techniques as a post-hoc analysis, we demonstrated the potential validity of individual rich club organizations (supplementary figure 3) for the classification of first-episode schizophrenia patients (see supplementary methods). Recent findings have shown that functional connectome organization may be an important source of information to predict the conversion to psychosis in a high-risk population.[50] Future studies combining multi-modal neuroimaging features may facilitate the identification of schizophrenia and further improve psychiatric care.

Several comments regarding the used methods and results need to be addressed. First, examining first-episode schizophrenia patients, we obtained some distinct results compared to previous studies examining chronic schizophrenia[8–10] A decrease in SC-FC coupling was found in rich club connections in first-episode patients in our study, while an increase in SC-FC coupling in whole-brain connections has been observed in treated, chronic schizophrenia patients.[8] The heterogeneity of these findings could reflect the effects of medication and/or of the clinical history of the patients, but further investigation is warranted. Investigating the whole replication dataset (10 medication-naïve and 29 treated patients) did not reveal alterations in rich club SC-FC coupling (P = .102 for NOS and .113 for SD). A second comment concerns the use of diffusion-weighted MRI and deterministic tractography to reconstruct cortico-cortical white matter pathways, as these methods are well-known to have several caveats regarding the reconstruction of complex oriented pathways.[51] We used a common clinical DWI protocol with a single b-value of 1000 s/mm^2, which might be insufficient to resolve complex crossing fibers in the tractography.[35,52,53] The use of higher magnetic field strength, higher b-value, more diffusion directions, and methods suitable for the reconstruction of complex fiber orientations (e.g.,

probabilistic tractography[54] or constrained spherical deconvolution[52,53]) may result in better reconstruction of white matter fiber pathways. Third, head movements during fMRI acquisition have been argued to be an important source of spurious signals in functional connectivity studies.[27,55] In this study, we performed scrubbing to reduce the effect of head motion, and including the head movement measures and number of scrubbed frames as covariates to the group-comparison statistical analyses revealed consistent findings (see supplementary results). Fourth, brain network architecture was characterized by means of graph theoretical metrics that have received large consensus in clinical connectome literature.[56–59] Nevertheless, it has been noted that graph metrics can be highly correlated in real-world networks[60] and new network measures are continuously proposed.[61,62] Future research applying advanced network measures could bring further insights into the characteristics of brain network alterations in early schizophrenia and the clinical diagnosis.

This study shows a reduced level of structural rich club connectivity in first-episode schizophrenia patients with no or limited medication history. We suggest that connectome features including rich club impairment reflect pathophysiological processes occurring early in the course of schizophrenia, independently from the medication history of the patients. Our results are important for advancing our understanding of the neuropathological mechanisms of first-episode schizophrenia. They add important empirical support for the use of individual connectome organization as a potential marker for disease classification.

Supplementary Material

Supplementary data are available at *Schizophrenia Bulletin* online.

Funding

Acknowledgments

References

1. Brugger SP, Howes OD. Heterogeneity and homogeneity of regional brain structure in schizophrenia: a meta-analysis. *JAMA Psychiatry.* 2017;74(11):1104–1111.

2. Dietsche B, Kircher T, Falkenberg I. Structural brain changes in schizophrenia at different stages of the illness: a selective review of longitudinal magnetic resonance imaging studies. *Aust N Z J Psychiatry.* 2017;51(5):500–508.

3. Dong D, Wang Y, Chang X, Luo C, Yao D. Dysfunction of large-scale brain networks in schizophrenia: a meta-analysis of resting-state functional connectivity. *Schizophr Bull.* 2018;44(1):168–181.

4. van den Heuvel MP, Mandl RC, Stam CJ, Kahn RS, Hulshoff Pol HE. Aberrant frontal and temporal complex network structure in schizophrenia: a graph theoretical analysis. *J Neurosci.* 2010;30(47):15915–15926.

5. van den Heuvel MP, Sporns O. Rich-club organization of the human connectome. *J Neurosci.* 2011;31(44):15775–15786.

6. Abraham A, Milham MP, Di Martino A, et al. Deriving reproducible biomarkers from multi-site resting-state data: an autism-based example. *Neuroimage.* 2017;147:736–745.

7. van den Heuvel MP, Kahn RS, Goñi J, Sporns O. High-cost, high-capacity backbone for global brain communication. *Proc Natl Acad Sci USA.* 2012;109(28):11372–11377.

8. van den Heuvel MP, Sporns O, Collin G, et al. Abnormal rich club organization and functional brain dynamics in schizophrenia. *JAMA Psychiatry.* 2013;70(8):783–792.

9. Yeo RA, Ryman SG, van den Heuvel MP, et al. Graph metrics of structural brain networks in individuals with schizophrenia and healthy controls: group differences, relationships with intelligence, and genetics. *J Int Neuropsychol Soc.* 2016;22(2):240–249.

10. Klauser P, Baker ST, Cropley VL, et al. White matter disruptions in schizophrenia are spatially widespread and topologically converge on brain network hubs. *Schizophr Bull.* 2017;43(2):425–435.

11. Crossley NA, Marques TR, Taylor H, et al. Connectomic correlates of response to treatment in first-episode psychosis. *Brain.* 2017;140(2):487–496.

12. Collin G, Kahn RS, de Reus MA, Cahn W, van den Heuvel MP. Impaired rich club connectivity in unaffected siblings of schizophrenia patients. *Schizophr Bull.* 2014;40(2):438–448.

13. Schmidt A, Crossley NA, Harrisberger F, et al. Structural network disorganization in subjects at clinical high risk for psychosis. *Schizophr Bull.* 2017;43(3):583–591.

14. Millan MJ, Andrieux A, Bartzokis G, et al. Altering the course of schizophrenia: progress and perspectives. *Nat Rev Drug Discov.* 2016;15(7):485–515.

15. Cui LB, Wang LX, Tian P, et al. Aberrant perfusion and its connectivity within default mode network of first-episode drug-naïve schizophrenia patients and their unaffected first-degree relatives. *Sci Rep.* 2017;7(1):16201.

16. Cui LB, Liu L, Wang HN, et al. Disease definition for schizophrenia by functional connectivity using radiomics strategy. *Schizophr Bull.* 2018;44(5):1053–1059.

17. Desikan RS, Ségonne F, Fischl B, et al. An automated labeling system for subdividing the human cerebral cortex on MRI scans into gyral based regions of interest. *Neuroimage.* 2006;31(3):968–980.

18. Cammoun L, Gigandet X, Meskaldji D, et al. Mapping the human connectome at multiple scales with diffusion spectrum MRI. *J Neurosci Methods.* 2012;203(2):386–397.

19. van den Heuvel MP, Scholtens LH, de Reus MA, Kahn RS. Associated microscale spine density and macroscale connectivity disruptions in schizophrenia. *Biol Psychiatry.* 2016;80(4):293–301.

20. Andersson JL, Skare S. A model-based method for retrospective correction of geometric distortions in diffusion-weighted EPI. *Neuroimage.* 2002;16(1):177–199.

21. Yeh FC, Wedeen VJ, Tseng WY. Generalized q-sampling imaging. *IEEE Trans Med Imaging.* 2010;29(9):1626–1635.

22. Chang LC, Jones DK, Pierpaoli C. RESTORE: robust estimation of tensors by outlier rejection. *Magn Reson Med.* 2005;53(5):1088–1095.

23. Mori S, van Zijl PC. Fiber tracking: principles and strategies - a technical review. *NMR Biomed.* 2002;15(7–8):468–480.

24. Sarwar T, Ramamohanarao K, Zalesky A. Mapping connectomes with diffusion MRI: deterministic or probabilistic tractography? *Magn Reson Med.* 2019;81(2):1368–1384.

25. van den Heuvel MP, de Reus MA, Feldman Barrett L, et al. Comparison of diffusion tractography and tract-tracing measures of connectivity strength in rhesus macaque connectome. *Hum Brain Mapp.* 2015;36(8):3064–3075.

26. Shen K, Goulas A, Grayson DS, et al. Exploring the limits of network topology estimation using diffusion-based tractography and tracer studies in the macaque cortex. *Neuroimage.* 2019;191:81–92. doi:10.1016/j.neuroimage.2019.02.018.

27. Power JD, Barnes KA, Snyder AZ, Schlaggar BL, Petersen SE. Spurious but systematic correlations in functional connectivity MRI networks arise from subject motion. *Neuroimage.* 2012;59(3):2142–2154.

28. Hagmann P, Cammoun L, Gigandet X, et al. Mapping the structural core of human cerebral cortex. *PLoS Biol.* 2008;6(7):e159.

29. van Wijk BC, Stam CJ, Daffertshofer A. Comparing brain networks of different size and connectivity density using graph theory. *PLoS One.* 2010;5(10):e13701.

30. van den Heuvel MP, de Lange SC, Zalesky A, Seguin C, Yeo BTT, Schmidt R. Proportional thresholding in resting-state fMRI functional connectivity networks and consequences for patient-control connectome studies: Issues and recommendations. *Neuroimage.* 2017;152:437–449.

31. Rubinov M, Sporns O. Complex network measures of brain connectivity: uses and interpretations. *Neuroimage.* 2010;52(3):1059–1069.

32. Opsahl T, Colizza V, Panzarasa P, Ramasco JJ. Prominence and control: the weighted rich-club effect. *Phys Rev Lett.* 2008;101(16):168702.

33. Zhu J, Wang C, Liu F, Qin W, Li J, Zhuo C. Alterations of functional and structural networks in schizophrenia patients with auditory verbal hallucinations. *Front Hum Neurosci.* 2016;10:114.

34. Collin G, Scholtens LH, Kahn RS, Hillegers MHJ, van den Heuvel MP. Affected anatomical rich club and structural-functional coupling in young offspring of schizophrenia and bipolar disorder patients. *Biol Psychiatry.* 2017;82(10):746–755.

35. Weiss C, Tursunova I, Neuschmelting V, et al. Improved nTMS- and DTI-derived CST tractography through anatomical ROI seeding on anterior pontine level compared to internal capsule. *Neuroimage Clin.* 2015;7:424–437.

36. Kelly S, Jahanshad N, Zalesky A, et al. Widespread white matter microstructural differences in schizophrenia across

4322 individuals: results from the ENIGMA Schizophrenia DTI Working Group. *Mol Psychiatry.* 2018;23(5):1261–1269.

37. Xiao Y, Sun H, Shi S, et al. White matter abnormalities in never-treated patients with long-term schizophrenia. *Am J Psychiatry.* 2018;175(11):1129–1136.

38. Caprihan A, Jones T, Chen H, et al. The paradoxical relationship between white matter, psychopathology and cognition in schizophrenia: a diffusion tensor and proton spectroscopic imaging study. *Neuropsychopharmacology.* 2015;40(9):2248–2257.

39. Xi YB, Guo F, Li H, et al. The structural connectivity pathology of first-episode schizophrenia based on the cardinal symptom of auditory verbal hallucinations. *Psychiatry Res Neuroimaging.* 2016;257:25–30.

40. Asmal L, du Plessis S, Vink M, Fouche JP, Chiliza B, Emsley R. Insight and white matter fractional anisotropy in first-episode schizophrenia. *Schizophr Res.* 2017;183:88–94.

41. Subramaniam K, Gill J, Fisher M, Mukherjee P, Nagarajan S, Vinogradov S. White matter microstructure predicts cognitive training-induced improvements in attention and executive functioning in schizophrenia. *Schizophr Res.* 2018;193:276–283.

42. Greicius MD, Kiviniemi V, Tervonen O, et al. Persistent default-mode network connectivity during light sedation. *Hum Brain Mapp.* 2008;29(7):839–847.

43. van den Heuvel MP, Mandl RC, Kahn RS, Hulshoff Pol HE. Functionally linked resting-state networks reflect the underlying structural connectivity architecture of the human brain. *Hum Brain Mapp.* 2009;30(10):3127–3141.

44. Marín O. Developmental timing and critical windows for the treatment of psychiatric disorders. *Nat Med.* 2016;22(11):1229–1238.

45. Silbereis JC, Pochareddy S, Zhu Y, Li M, Sestan N. The cellular and molecular landscapes of the developing human central nervous system. *Neuron.* 2016;89(2):248–268.

46. APA. *Diagnostic and Statistical Manual of Mental Disorders.* 5th ed. Washington, DC: American Psychiatric Association; 2013:87–118.

47. Gillies RJ, Kinahan PE, Hricak H. Radiomics: images are more than pictures, they are data. *Radiology.* 2016;278(2):563–577.

48. Aerts HJ, Velazquez ER, Leijenaar RT, et al. Decoding tumour phenotype by noninvasive imaging using a quantitative radiomics approach. *Nat Commun.* 2014;5:4006.

49. Wolfers T, Doan NT, Kaufmann T, et al. Mapping the heterogeneous phenotype of schizophrenia and bipolar disorder using normative models. *JAMA Psychiatry.* 2018;75(11):1146–1155.

50. Collin G, Seidman LJ, Keshavan MS, et al. Functional connectome organization predicts conversion to psychosis in clinical high-risk youth from the SHARP program. *Mol Psychiatry.* 2018. doi: 10.1038/s41380-018-0288-x.

51. Jbabdi S, Johansen-Berg H. Tractography: where do we go from here? *Brain Connect.* 2011;1(3):169–183.

52. Tournier JD, Calamante F, Connelly A. Robust determination of the fibre orientation distribution in diffusion MRI: non-negativity constrained super-resolved spherical deconvolution. *Neuroimage.* 2007;35(4):1459–1472.

53. Tournier JD, Calamante F, Gadian DG, Connelly A. Direct estimation of the fiber orientation density function from diffusion-weighted MRI data using spherical deconvolution. *Neuroimage.* 2004;23(3):1176–1185.

54. Behrens TE, Berg HJ, Jbabdi S, Rushworth MF, Woolrich MW. Probabilistic diffusion tractography with multiple fibre orientations: What can we gain? *Neuroimage.* 2007;34(1):144–155.

55. Yan CG, Cheung B, Kelly C, et al. A comprehensive assessment of regional variation in the impact of head micromovements on functional connectomics. *Neuroimage.* 2013;76:183–201.

56. Fornito A, Bullmore ET. Connectomics: a new paradigm for understanding brain disease. *Eur Neuropsychopharmacol.* 2015;25(5):733–748.

57. van den Heuvel MP, Fornito A. Brain networks in schizophrenia. *Neuropsychol Rev.* 2014;24(1):32–48.

58. Griffa A, Baumann PS, Thiran JP, Hagmann P. Structural connectomics in brain diseases. *Neuroimage.* 2013;80:515–526.

59. Fornito A, Zalesky A, Pantelis C, Bullmore ET. Schizophrenia, neuroimaging and connectomics. *Neuroimage.* 2012;62(4):2296–2314.

60. Sporns O, Honey CJ, Kötter R. Identification and classification of hubs in brain networks. *PLoS One.* 2007;2(10):e1049.

61. Bertolero MA, Yeo BTT, D'Esposito M. The diverse club. *Nat Commun.* 2017;8(1):1277.

62. Betzel RF, Bassett DS. Multi-scale brain networks. *Neuroimage.* 2017;160:73–83.